J. Biochem. 2008;144(6)789–798
doi:10.1093/jb/mvn132

Isolation and Biochemical Characterization of Two Forms of RD21 from Cotyledons of Daikon Radish (*Raphanus sativus*)

Yayoi Kikuchi, Hiroko Saika, Keizo Yuasa, Masami Nagahama and Akihiko Tsuji*
Department of Biological Science and Technology, The University of Tokushima Graduate School, 2-1 Minamijosanjima, Tokushima 770-8506, Japan

Received August 27, 2008; accepted September 27, 2008; published online October 6, 2008

RD21 (Responsive to desiccation-21) is an *Arabidopsis* cysteine protease which possesses a granulin-like domain at the C-terminus. Although two forms of RD21 have been identified, consisting of an intermediate form (iRD21) containing a granulin domain and a mature form (mRD21) lacking this domain, the enzymatic properties of these enzymes remain poorly understood. In this study, mRD21 orthologue was purified to homogeneity from the cotyledons of daikon radish (*Raphanus sativus*). RD21 preferentially cleaved peptide bond that had an aromatic or hydrophobic amino acid at the P2 position. Furthermore, the presence of a polar amino acid at the P1 position enhanced the cleavage susceptibility of the peptide bond, although the importance of the type of amino acid residue at the P1 and P1′ positions was not as significant as the residue located at the P2 position. The iRD21 was also identified as an oligomeric form by gel filtration and sedimentation analyses. The expression of RD21 mRNA was initiated by imbibition and continued at almost constant levels during germination. On the other hand, the enzyme activity increased markedly 5 days after imbibition. These results indicate that this elevation of RD21 activity is generated post-transcriptionally.

Key words: cleavage specificity, cysteine protease, germination, granulin domain, RD21.

Abbreviations: ACTH, adrenocorticotropic hormone; *Boc*, *t*-butyloxycarbonyl; CA074, [*N*-(L-*3-trans*-propyl-carbamoyl-oxirane-2-carbonyl)-L-isoleucyl-L-proline]; E-64, *trans*-epoxysuccinyl-L-leucylamide-(4-guanidino)-butane; *Glt*, glutaryl; MCA,4-methylcoumaryl 7-amide; PMSF, phenylmethanesulfonyl fluoride; PVDF, polyvinylidene fluoride; *pyr*, L-pyroglutamyl; RD21, responsive to desiccation-21; TLCK, *Nα-p*-tosyl-L-lysine chloromethyl ketone; *Z*, carbobenzoxy.

Plant cysteine proteases are involved in several physiological processes including the processing of storage proteins into mature forms (*1–4*) and the liberation of amino acids required for seed germination (*5*). In general, the expression of cysteine proteases during germination is regulated by gibberellin, which is subsequently secreted into the endosperm where storage proteins undergo degradation. Several cysteine proteases have been purified from seeds, some of which are known to degrade storage proteins (*6–11*). Recently, plant cysteine proteases were shown to play important roles in intracellular protein catabolism for senescence, programmed cell death and plant resistance against pathogens or insects (*12–16*).

Arabidopsis responsive to desiccation-21 (RD21) is a cysteine protease belonging to the papain family. RD21 cDNA was identified as a putative stress-induced responsive gene following dehydration in *Arabidopsis* (*17*). RD21 was also induced by leaf senescence and high salt conditions (*18*, *19*). RD21 is localized in the vacuole, a major compartment involved in protein degradation. Unlike other members of the papain family, RD21 has a C-terminal extension sequence composed of a 2 kDa proline-rich domain and a 10 kDa granulin domain that has high homology to the animal epithelial/granulin family of proteins. RD21 is synthesized as a pro-protein of 57 kDa that is processed via an intermediate of 38 kDa (iRD21) into a mature protein of 33 kDa (mRD21) (*20*). Hayashi *et al*. (*21*) showed that prior to removal of the C-terminal granulin domain, iRD21 accumulated in the endoplasmic reticulum (ER) bodies of epidermal cells. The ER bodies were specifically located in the epidermal cells in healthy seedlings. When seedlings were stressed, the ER bodies began to fuse with the vacuoles (*21*). These data imply that iRD21 is transported directly from the ER bodies into the vacuoles, and through removal of the C-terminal granulin domain iRD21 slowly matures into an active and soluble protease (*20*, *21*). The enzymatic properties of RD21 have not been clarified.

In this study, we purified RD21 from daikon cotyledons and the enzyme cleavage specificity was investigated. This is the first report detailing the isolation and enzymatic characterization of RD21.

MATERIALS AND METHODS

Materials—Peptide 4-methylcoumaryl 7-amide (MCA) substrate, human dynorphin A, angiotensin IV, methionine-enkephalin, glucagon, adrenocorticotropic

*To whom correspondence should be addressed. Tel: +81-88-656-7526, Fax: +81-88-655-3161, E-mail: tsuji@bio.tokushima-u.ac.jp

hormone (ACTH), leupeptin, E-64, chymostatin and CA074 ([*N*-(L-3-*trans*-propylcarbamoyl-oxirane-2-carbonyl)-L-isoleucyl-L-proline]) were purchased from the Peptide Institute (Osaka, Japan). Sephacryl S-200 was from GE Healthcare (Uppsala, Sweden). Egg cystatin was purified by the method of Anastosi *et al*. (*22*) and immobilized onto Sepharose 4B (*23*). All other chemicals used were of analytical grade.

Plant Material—Fresh sprouts of daikon radish (*Raphanus sativus*) grown by hydroponics were purchased from a grocery store and cotyledons were used for purification of the enzyme. For the analysis of enzyme expression, daikon radish seeds were obtained from Nakahara Seed Product Co. Ltd (Fukuoka, Japan). Daikon radish seeds were allowed to imbibe water on filter paper at 20°C in the dark. After 2 days, embryos were grown at 20°C under long-day conditions (16 h light, 8 h dark) until collection.

Enzyme Assay—Protease activity was assayed using carbobenzoxy-Phe-Arg-4-methylcoumaryl 7-amide (Z-Phe-Arg-MCA). The reaction mixture contained 0.1 M acetate buffer (pH 5.5) and 50 μM Z-Phe-Arg-MCA. The reaction was initiated by addition of enzyme solution. Following incubation at 37°C for 10–30 min, the reaction was terminated and the MCA liberated was detected fluorometrically as previously described (*24*). Protein concentration was determined by the Bradford method using BSA as a standard (*25*).

Purification of Enzyme from Cotyledons of Daikon Radish—All purification procedures were performed at 4°C unless otherwise indicated. One kilogram of daikon radish cotyledons were homogenized with 5 l of ice-cold 20 mM acetate buffer (pH 6.5) containing 0.5 mM EDTA and 1mM β-mercaptoethanol (buffer A) using a Waring blender. The homogenate was centrifuged at 12,000*g* for 10 min at 4°C. The supernatant was fractionated with ammonium sulfate (60% saturation). The precipitate was dissolved in buffer A and dialysed overnight at 4°C against buffer A. Following centrifugation at 12,000*g* for 10 min at 4°C, the resultant supernatant was concentrated by ultrafiltration (Amicon YM-10 filter) and then applied to a DEAE-cellulose column (7.0 × 25 cm) equilibrated with buffer A. The column was washed with buffer A containing 0.1 M NaCl. Z-Phe-Arg-MCA cleaving activity was eluted using a linear gradient of NaCl (0.1–0.5 M) in buffer A. Fractions with activity were concentrated by ultrafiltration. The concentrate was applied to a Sephacryl S-200 gel filtration column (2.5 × 100 cm) equilibrated with buffer A containing 0.1 M NaCl. Fractions with activity were concentrated and applied to a hydroxyapatite column (0.8 × 2 cm). Bound proteins were eluted using a linear gradient of sodium phosphate (0–0.2 M) in buffer A. Fractions with activity were concentrated and applied to a Superdex 200 PC 3.2/30 column (GE Healthcare, Uppsala, Sweden). The fraction with activity was used as the final preparation.

Sequence Analysis of RD21—Purified RD21 was subjected to SDS–PAGE (*26*) and then blotted onto a polyvinylidene fluoride (PVDF) membrane (Immobilon^{TM}, 0.45 μm Millipore, Bedford, MA, USA) according to the manufacturer's instructions. The protein band detected using Ponceau S was cut into small pieces and then applied to an automated protein sequencer (Shimadzu PPSQ-10, Kyoto, Japan).

Cloning of Daikon Radish RD21 Catalytic Domain—cDNA encoding the catalytic domain of RD21 was cloned by PCR. A sense primer was designed using the purified daikon radish RD21 N-terminal amino acid sequence (DAIPESVDWR) and an antisense primer was designed using the *Arabidopsis* RD21 sequence. The sequences of the sense and antisense primers were 5′-GATGCCATCC CGGAGTCTGTCGACTGGAG-3′ and 5′-CGGGTACTCGT GAGGGCAGCAACT-3′, respectively. Total RNA was isolated from cotyledons of daikon radish (5 days after imbibition) using TRIZOL reagent (Invitrogen, Carlsbad, CA, USA) according to the manufacturer's protocol. One microgram of total RNA was reverse-transcribed using M-MLV reverse transcriptase (WAKO, Osaka, Japan) with a random hexamer. PCR was carried out by 30 cycles of denaturation at 95°C for 30 s, annealing at 53°C for 30 s, and then followed by extension at 72°C for 1 min. The PCR product of the expected size (867 bp) was amplified and sequenced.

Cleavage Specificity Analysis—Two nanomoles of peptide substrate (dynorphin A, angiotensin IV, methionine-enkephalin, glucagon and ACTH) was dissolved in 0.1 M acetate buffer (pH 5.5) and incubated with purified mRD21 (3.5 pmol) at 37°C. After 5 h or 16 h, the reaction mixtures were lyophilized and dissolved in 0.1% trifluoroacetic acid. The peptides were purified by reversed phase (RP)-HPLC on an mRPC C2/C18 pc3.2/3 column (GE Healthcare, Uppsala, Sweden). Purified peptide fragments were applied to glass fiber discs that had been coated with polybrene and then analysed using an automated protein sequencer. Bovine β-casein (5 nmol) was digested with mRD21 (20 pmol) at 37°C for 6 h. Digested fragments were separated by SDS–PAGE (15%), transferred onto a PVDF membrane and N-terminal sequences were analysed using an automated protein sequencer.

Sedimentation Velocity Analysis—RD21 was purified from 100 g of cotyledons by ammonium sulfate fractionation and DEAE-cellulose chromatography as mentioned above. Purified RD21 was fractionated by sedimentation on a 5–20% sucrose gradient for 17 h at 4°C using an SW41 rotor at 35,000 r.p.m. Individual fractions (0.5 ml) were analysed by cystatin-sepharose chromatography (*23*). The beads was washed five times by centrifugation using buffer A containing 0.1 M NaCl and 0.5% Triton X-100. Finally, the beads were suspended in 50 μl of loading buffer and treated at 95°C for 5 min. Sample (10 μl) was subjected to SDS–PAGE and the gel was stained with Coomassie brilliant blue (CBB). The remaining sample was used for sequence analysis. Catalase (240 kDa) and aldolase (158 kDa) were used as internal size standards.

RT-PCR Analysis of the RD21—The expression of RD21 transcripts in cotyledons (1, 2, 3, 4, 5, 6 and 8 days after imbibition and dry seeds before imbibition) were analysed by RT-PCR as mentioned above. Actin-2 transcript was amplified by PCR using sense primer 5′-GCTGTTCTC TCCCTGTACGCCAGTG-3′, corresponding to nucleotides 418–442 of *Arabidopsis* actin-2 cDNA (DDBJ accession number AY096381), and antisense primer 5′-CCAGCAGC TTCCATTCCCACGAAC-3′, corresponding to nucleotides

801–824 of *Arabidopsis* actin-2 cDNA (DDBJ accession number AY096381). PCR was carried out for 28 cycles (95°C, 30 s; 53°C, 30 s; and 72°C, 30 s), and identification of the PCR products was confirmed by sequencing.

Analysis of RD21 Activity during Germination—One hundred grams of daikon cotyledons (3, 5 and 8 days after imbibition) was homogenized in 500 ml buffer A. The homogenate was fractionated using ammonium sulfate (60% saturation) and then subjected to DEAE-cellulose column chromatography. The activity was eluted with buffer A containing 0.05 M, 0.15 M or 0.4 M NaCl. The activity was detected using the synthetic substrates Z-Phe-Arg-MCA and Boc-Leu-Arg-Arg-MCA.

RESULTS

Purification of RD21—The Z-Phe-Arg-MCA cleaving activity in cotyledons from daikon radish was eluted as three peaks with DEAE-cellulose column chromatography (Fig. 1A). The third peak with activity eluted with a linear gradient of NaCl was completely inhibited by E-64. The Z-Phe-Arg-MCA cleaving activity in the third peak was further separated into two peaks with Sephacryl S-200 gel filtration chromatography (Fig. 1B). Both Z-Phe-Arg-MCA cleaving activities were E-64-sensitive. The activity eluted at a position corresponding to 30 kDa (c fraction) was further purified by employing a series of column chromatographic procedures utilizing hydroxyapatite and Superdex 200. Table 1 summarizes the results of a typical purification of the 30 kDa cysteine protease. From 1 kg of daikon radish cotyledons, 2.2 μg of purified enzyme was obtained. As shown in Fig. 2A, the purified enzyme yielded a single protein band corresponding to a molecular mass of 30 kDa. In an effort to characterize the daikon cysteine proteases at the amino acid level, the N-terminal sequence of the 30 kDa protein band was examined. The N-terminal sequence (DAIPESVDWRKE) of the 30 kDa protein showed the highest degree of identity with the amino terminal sequence DELPESIDWRKK,

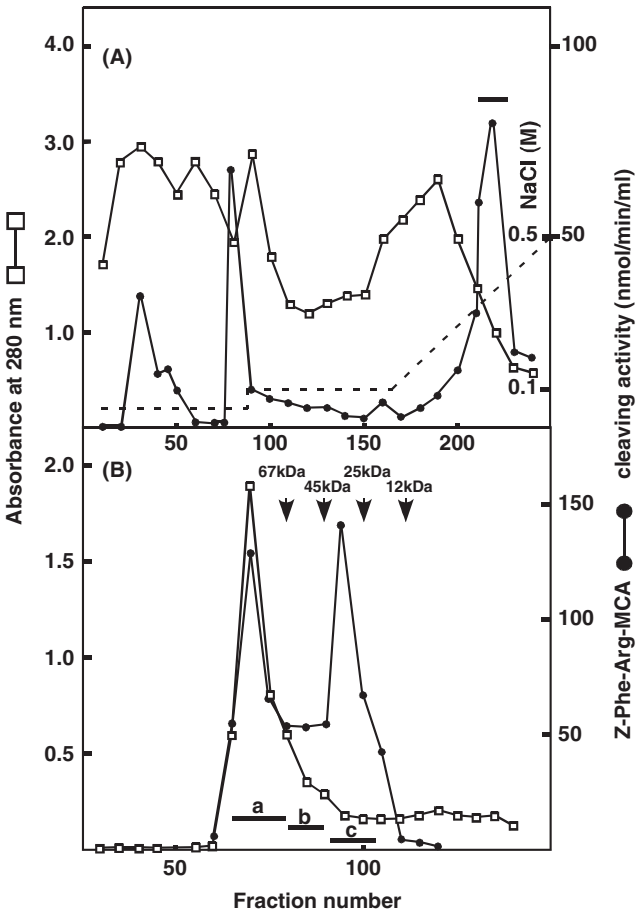

Fig. 1. **Purification of daikon radish RD21 by column chromatography.** (A) DEAE-cellulose chromatography. (B) Sephacryl S-200 gel filtration. The column chromatography was carried out as described under MATERIALS AND METHODS section. The fractions indicated by the horizontal bar were pooled and concentrated.

Table 1. **Purification of RD21 from daikon radish cotyledons.**

Steps	Total protein (mg)	Activity (μmol min^{-1})	Activity (μmol min^{-1} mg^{-1})	Yield (%)	Purification (fold)
Crude extract	6,213	81.6	0.013	100	1
Ammonium sulfate	1,066	17.9	0.017	21.9	1.3
DEAE-cellulose	14.0	3.19	0.228	3.91	17.5
Sephacryl S-200	0.30	0.820	2.73	1.00	210
Hydroxyapatite	0.025	0.130	5.20	0.16	400
Superdex 200	0.0022[a]	0.031	14.1	0.038	1,085

[a]The amount of protein was estimated by the absorbance at 280 nm.

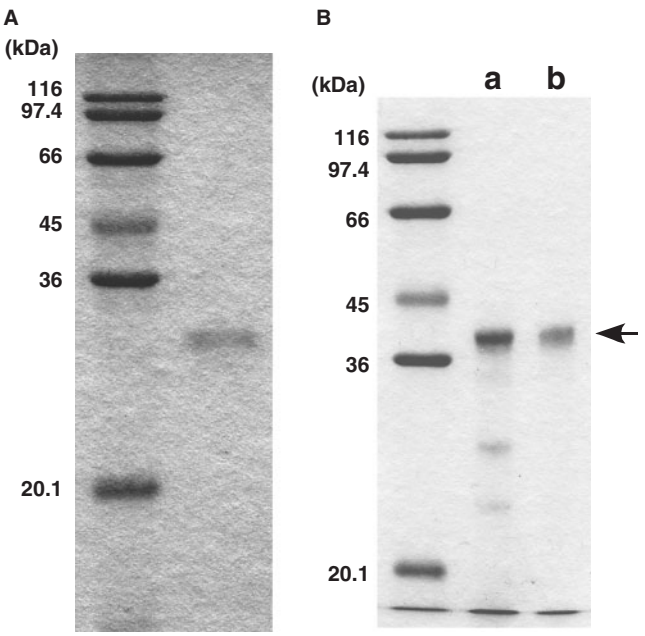

Fig. 2. **SDS–PAGE of purified daikon mRD21 and iRD21.** (A) Purified mRD21 was resolved using a 12% gel. Protein was detected using CBB. (B) iRD21 in the a and b fractions obtained from gel filtration (Fig. 1B) was incubated with cystatin-sepharose. Proteins bound to cystatin-sepharose were analysed by SDS–PAGE (12% gel). The 40 kDa major protein bands were indicated by arrow.

corresponding to amino acid residues 135–146 as predicted from the cDNA (DDBJ accession number AY072130) of the *Arabidopsis* RD21A cysteine protease. Twelve N-terminal amino acid residues of the 30 kDa purified enzyme exhibited 100% identity with amino acid sequences of the broccoli RD21 orthologue BoCP3, identified as a dehydration-responsive cysteine protease.

Isolation of cDNA Encoding the Catalytic Domain of Daikon Radish RD21—To confirm the identity of the daikon 30 kDa cysteine protease, cDNA encoding the 30 kDa enzyme was cloned by PCR using primers corresponding to the N-terminal residue 1–10 (DAIPESVDWR) and conserved sequence of the granulin domain. A single PCR product with the expected size (867 bp) was amplified. The sequence ($K^{11}E^{12}$) of the 30 kDa protein, which follows the site for the sense primer, coincided with the deduced sequence (Fig. 3). The deduced sequence of the catalytic domain showed high amino acid identity with *Arabidopsis* RD21A (84%, DDBJ accession number AY072130). Alignment of the

```
   1  gatgccatcccggagtctgtcgactggaggaaagaaggtgccgtcgccgccgttaaagat   60
   1  D  A  I  P  E  S  V  D  W  R  K  E  G  A  V  A  A  V  K  D    20

  61  cagggaagctgcgggagctgttgggcattttcaacgattggggcagtggaaggaataaac  120
  21  Q  G  S  C  G  S  C  W  A  F  S  T  I  G  A  V  E  G  I  N    40

 121  aagatcgtgacaggagacttgatctctttgtctgaacaagaactggtcgactgtgacaca  180
  41  K  I  V  T  G  D  L  I  S  L  S  E  Q  E  L  V  D  C  D  T    60

 181  tcttacaaccaaggttgtaatggaggtttgatggattatgcgtttgagttcatcatcaaa  240
  61  S  Y  N  Q  G  C  N  G  G  L  M  D  Y  A  F  E  F  I  I  K    80

 241  aatggcggtattgataccgaagaggattatccatacaaagctgctgatggtcgttgtgat  300
  81  N  G  G  I  D  T  E  E  D  Y  P  Y  K  A  A  D  G  R  C  D   100

 301  cagaacaggaaaaacgcaaaggttgtcacaattgatgcgtatgaagatgttcctgagaac  360
 101  Q  N  R  K  N  A  K  V  V  T  I  D  A  Y  E  D  V  P  E  N   120

 361  aacgaggctgcgcttaagaaagctttggctaaccagcctattagtgttgccattgaagct  420
 121  N  E  A  A  L  K  K  A  L  A  N  Q  P  I  S  V  A  I  E  A   140

 421  ggtggtcgcgctttccagctctattcttcgggtgtatttgatggaacatgtggtacggag  480
 141  G  G  R  A  F  Q  L  Y  S  S  G  V  F  D  G  T  C  G  T  E   160

 481  ctagaccacggagttgtagcggttggttacggaactgagaacggaaaggactactggatt  540
 161  L  D  H  G  V  V  A  V  G  Y  G  T  E  N  G  K  D  Y  W  I   180

 541  gtgaggaactcatggggaggaagctggggagagagcggatacataaagatggcacgtaac  600
 181  V  R  N  S  W  G  G  S  W  G  E  S  G  Y  I  K  M  A  R  N   200

 601  attgcggaggcaactggaaagtgtggaatcgccatggaggcttcgtatccgatcaagaag  660
 201  I  A  E  A  T  G  K  C  G  I  A  M  E  A  S  Y  P  I  K  K   220

 661  ggtcagaacccgccacaacctggaccgtcaccaccgtctcccatcaagccaccgacccag  720
 221  G  Q  N  P  P  Q  P  G  P  S  P  P  S  P  I  K  P  P  T  Q   240

 721  tgtgacaaatactactcttgccctgaagggaacacttgctgttgtctcttcaagtacggc  780
 241  C  D  K  Y  Y  S  C  P  E  G  N  T  C  C  C  L  F  K  Y  G   260

 781  aagtactgcttcggttggggatgttgccctctggaagctgctacttgctgcgatgataac  840
 261  K  Y  C  F  G  W  G  C  C  P  L  E  A  A  T  C  C  D  D  N   280

 841  actagttgctgccctcacgagtacccg  867
 281  T  S  C  C  P  H  E  Y  P   289
```

Fig. 3. **Nucleotide sequence of the cDNA encoding the catalytic domain of RD21 and the deduced amino acid sequence.** The deduced amino acid sequence is displayed below the nucleotide sequence in one-letter code. The primer positions used for PCR are marked with bold lines. The active site residues Cys^{27}, His^{163} and Asn^{183} are shown in black boxes. The amino acid residues within the white box represent the putative proline-rich domain and the shaded amino acid residues represent the putative granulin-like domain. The potential glycosylation site is double-underlined. The nucleotide sequences of cDNA encoding the catalytic domain of daikon RD21 has been deposited in DDBJ under the accession number AB454126.

RD21 putative catalytic domain with *Arabidopsis* RD21 shows conservation of the catalytic residues Cys^{27}, His^{163} and Asn^{183} within this domain. One possible glycosylation site (Asn^{280}) was also identified.

Gel Filtration and Sedimentation Analyses of iRD21—With the gel filtration procedure (Fig. 1B), we found that Z-Phe-Arg-MCA cleaving activity eluted in high molecular weight corresponding to 95 kDa (a fraction) and 60 kDa (b fraction). Like the case with RD21, Z-Phe-Arg-MCA cleaving activities in a and b fractions were completely inhibited by E-64. Papain-like cysteine proteases in these fractions were isolated by cystatin-sepharose chromatography and SDS–PAGE (Fig. 2B). Most of the activity bound to the cystatin-sepharose. As shown in Fig. 2B, the major protein bound to cystatin-sepharose was identified both a (lane a) and b (lane b) fractions as a 40 kDa. The N-terminal nine amino acid residues (DAIPESVDW) of the 40 kDa protein from a and b fractions perfectly matched the sequence of the purified 30 kDa enzyme, although its molecular mass was 10 kDa larger than the purified 30 kDa enzyme. In *Arabidopsis*, RD21A is known to exist as two forms, a 38 kDa intermediate form containing C-terminal granulin domain and 33 kDa mature form in which granulin domain has been removed (*20*). Our results suggest that the 40 and 30 kDa cysteine proteases identified in daikon radish correspond to the 38 kDa (intermediate) and 33 kDa (mature) forms of *Arabidopsis* RD21A cysteine proteases, respectively. The *Arabidopsis* iRD21 accumulated in the vacuoles in aggregate form (*20*). It is highly likely that daikon 40 kDa iRD21 also aggregates like *Arabidopsis* iRD21 as shown in Fig. 2B. The molecular size of the iRD21 and mRD21 proteins obtained from DEAE-cellulose chromatography was further analysed by sucrose density gradient centrifugation (Fig. 4). The content of the 40 kDa iRD21 protein was greater than that of the 30 kDa mRD21 protein. The 40 kDa iRD21 protein sedimented as trimer and tetramer aggregates. The Z-Phe-Arg-MCA cleaving activity peak (number 19) is coincident with that of the 30 kDa mRD21 protein; whereas, the shoulder of the activity sedimented faster than that of the 30 kDa mRD21 protein which overlapped with the sedimentation pattern of the 40 kDa iRD21 protein. These results suggest that the 40 kDa iRD21 protein possesses Z-Phe-Arg-MCA cleaving activity.

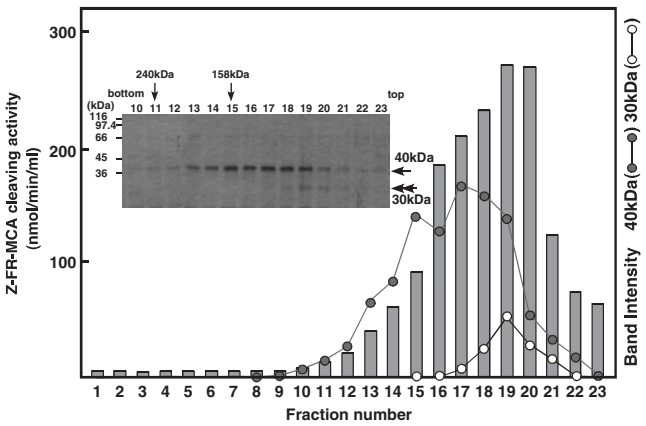

Fig. 4. **Sedimentation velocity analysis of iRD21 and mRD21.** The RD21 fraction obtained from DEAE-cellulose column chromatography was fractionated on a 5–20% sucrose gradient for 17 h. Individual fractions was assayed for Z-Phe-Arg-MCA cleaving activity. Individual gradient fractions were analysed by cystatin-sepharose and SDS–PAGE as described under MATERIALS AND METHODS section. Identities of iRD21 and mRD21 were confirmed by amino acid sequences of 40 kDa and 30 kDa bands. The intensity of the 40 kDa band (closed circle) and the 30 kDa band (open circle) was quantified using NIH image software.

Cleavage Specificity towards Various Synthetic Substrates—The effect of pH on the activity of mRD21 was examined. The enzyme showed highest activity at pH 4.5. The activity of purified daikon mRD21 towards various synthetic substrates is shown in Fig. 5. mRD21 hydrolysed Z-Phe-Arg-MCA, Boc-Val-Leu-Lys-MCA and Z-Arg-Arg-MCA. The tri- or tetra-peptide substrates possessing a dibasic amino acid at the P1 and P2 positions (Arg-Arg and Lys-Arg) were not good substrates for mRD21. The tri- or tetra-peptide substrate possessing a Gly (Boc-Ile-Glu-Gly-Arg-MCA) or Ser (Boc-Phe-Ser-Arg-MCA) residue at the P2 position was not effectively hydrolysed. These results suggest that P2 residues in the substrate are important in determining the catalytic efficiency of the enzyme. The k_{cat}/K_m values of Z-Phe-Arg-MCA, Boc-Val-Leu-Lys-MCA and Z-Arg-Arg-MCA were 1.4×10^6, 0.5×10^6 and $1.0 \times 10^6\,M^{-1}s^{-1}$, respectively. The K_m values (Z-Phe-Arg-MCA: $6.1 \pm 0.49\,\mu M$, Boc-Val-Leu-Lys-MCA: $5.2 \pm 0.09\,\mu M$ and Z-Arg-Arg-MCA: $7.8 \pm 0.27\,\mu M$) were almost identical. As shown in Fig. 2B, b fraction obtained from Sephacryl S-200 chromatography contained an iRD21 as a papain-like cysteine protease and other cystatin-binding proteins were not found. Therefore, cleavage specificity of iRD21 towards synthetic substrates was identified using b fraction. Similarly, like mRD21, iRD21 efficiently hydrolysed Z-Phe-Arg-MCA (K_m: $16.3 \pm 0.80\,\mu M$), Boc-Val-Lys-Arg-MCA (K_m: $27.9 \pm 1.97\,\mu M$) and Z-Arg-Arg-MCA (K_m: $13.8 \pm 0.29\,\mu M$), although the K_m values were 2- to 5-fold higher than those for mRD21.

Hydrolysis of Angiotensin IV, Methionine-enkephalin and Dynorphin A—The ability of mRD21 to hydrolyse

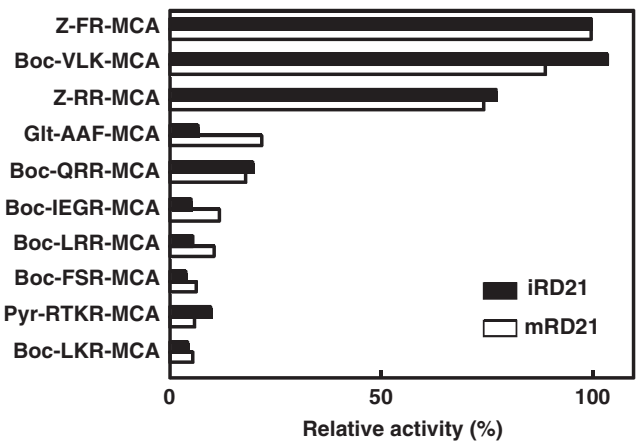

Fig. 5. **Cleavage specificity of mRD21 and iRD21 towards synthetic substrates.** Enzyme activity was determined in 0.1 M acetate buffer (pH 5.5) using various substrates at a concentration of 50 μM.

model peptides including angiotensin IV, methionine-enkephalin and dynorphin A was examined. These peptides were digested using mRD21 at 37°C for 16 h. Cleavage of angiotensin IV yielded three peptides which were separated by RP-HPLC (Fig. 6A) and amino acid sequences were determined. Cleavage occurred on the carboxyl side of Tyr^2 and Ile^3. Methionine-enkephalin and dynorphin A were also digested using mRD21 (Fig. 6B and C). The carboxyl side of Gly^2 of methionine-enkephalin was cleaved. Digestion of dynorphin A generated eight peptides. Fig. 6D shows the mRD21 cleavage sites of these peptides. mRD21 showed broad cleavage specificity, where cleavage occurred on the carboxyl side of Try, Ile, Gly, Arg, Lys and Leu. On the other hand, the P2 position of the cleavage site of angiotensin IV and methionine-enkephalin was occupied by Val^1, Tyr^2 and Tyr^1, respectively. In dynorphin A, the P2 position of the cleaved bonds Gly^2–Gly^3, Arg^6–Arg^7 and Arg^9–Pro^{10} was occupied by Try^1, Leu^5 and Ile^8, respectively. Peptides 5 and 6 were major products following digestion of dynorphin A by mRD21. These results indicate that mRD21 prefers hydrophobic or aromatic amino acids at the P2 position, although the enzyme showed broad cleavage specificity.

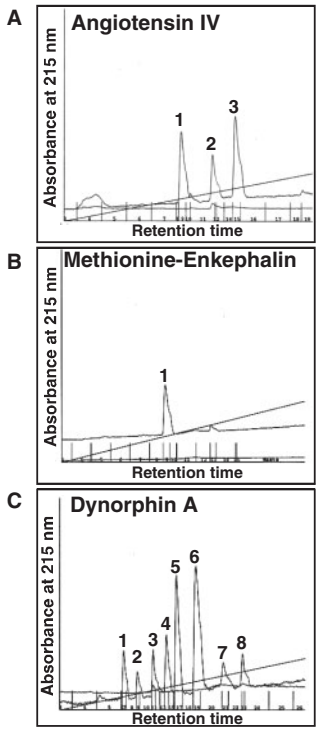

D

	P3	P2	P1	P'1	P'2
Angiotensin IV		V	Y	I	H
	V	Y	I	H	P
Methionine-Enkephalin		Y	G	G	F
Dynorphin A		Y	G	G	F
	F	L	R	R	I
	L	R	R	I	R
	R	R	I	R	P
	R	I	R	P	K
	R	P	K	L	K
	P	K	L	K	

Fig. 6. **Cleavage of angiotensin IV, methionine-enkephalin and dynorphin A by mRD21.** HPLC profiles of digested angiotensin IV (A), methionine-enkephalin (B) and dynorphin A (C) following cleavage using mRD21. Peaks were collected and sequenced. The amino acid sequences (one-letter code) of the peptides are shown (D). The major cleavage sites are indicated by arrows. The arrow in parenthesis indicates a minor cleavage site.

Hydrolysis of Glucagon, ACTH and β-Casein—To confirm the cleavage specificity of mRD21, glucagon and ACTH were also digested using mRD21 and cleaved sites were determined. Analysis of the products following 5 h incubation led to the identification of three glucagon-derived peptides (His^1–Thr^7, Ser^8–Asp^{15} and Trp^{25}–Thr^{29}) and five ACTH-derived peptides (Ser^1–Arg^8, Trp^9–Val^{13}, Trp^9–Gly^{14}, Lys^{15}–Lys^{21} and Val^{22}–Pro^{24}). The glucagon Ser^{16}–Gln^{24} peptide was not identified, suggesting that the peptide was further digested into small peptides or amino acids by RD21. As shown in Fig. 7, the major cleavage sites within glucagon were located at bonds Thr^7–Ser^8, Asp^{15}–Ser^{16} and Gln^{24}–Trp^{25}. ACTH was cleaved at Arg^8–Trp^9, Gly^{14}–Lys^{15} and Lys^{21}–Val^{22}. The Ser^3–Met^4 bond of ACTH was identified as a minor cleavage site. Bovine β-casein was digested using the purified enzyme at pH 5.5 for 6 h. The four major fragments (20, 18, 16 and 11 kDa) generated were separated by SDS–PAGE (data not shown), transferred onto a PVDF membrane and then sequenced. The N-terminal sequence (four residues) of the 20 and 18 kDa fragments is Arg-Glu-Leu-Glu, which corresponds to the N-terminal sequence of mature β-casein. Two N-terminal sequences (Arg-Glu-Leu-Glu and Gln-Thr-Pro-Val) were identified in the 16 kDa fragment. The N-terminal sequence of the 10 kDa fragment was Glu-Ala-Met-Ala. Gln-Thr-Pro-Val and Glu-Ala-Met-Ala correspond to amino acid numbers 79–82 and 100–103, respectively. Cleavage at Leu-Thr-↓-Gln^{79} and Val-Lys-↓-Glu^{100} was evident (Fig. 7). These results confirm that mRD21 preferentially hydrolyses peptide bonds which possess aromatic or hydrophobic residues at the position P2.

Effect of Protease Inhibitors—The effect of inhibitors on the activity of mRD21 and iRD21 was examined (Table 2). Both enzymes were strongly inhibited by leupeptin, antipain, E-64 and cystatin. In contrast, phenylmethanesulfonyl fluoride (PMSF), *o*-phenanthroline and EDTA had no significant effect on both mRD21 and iRD21 activities. Compared with cathepsin B, mRD21 and iRD21 are less sensitive to CA074; whereas, both enzymes are partially inhibited by chymostatin and *Nα-p*-tosyl-L-lysine chloromethyl ketone (TLCK).

RD21 Expression During Germination—In an effort to delineate the role of RD21 during germination, the expression of RD21 in the cotyledons of germinating embryo was analysed at both the mRNA and enzyme activity levels (Fig. 8). RD21 transcript was first analysed by RT-PCR, with actin-2 being used as an internal standard. As shown in Fig. 8C, RD21 transcript was not detected in cotyledons from dormant seeds, and expression of RD21 mRNA was initiated by imbibition. The expression level of RD21 mRNA was almost constant during germination (1–5 days) and then decreased.

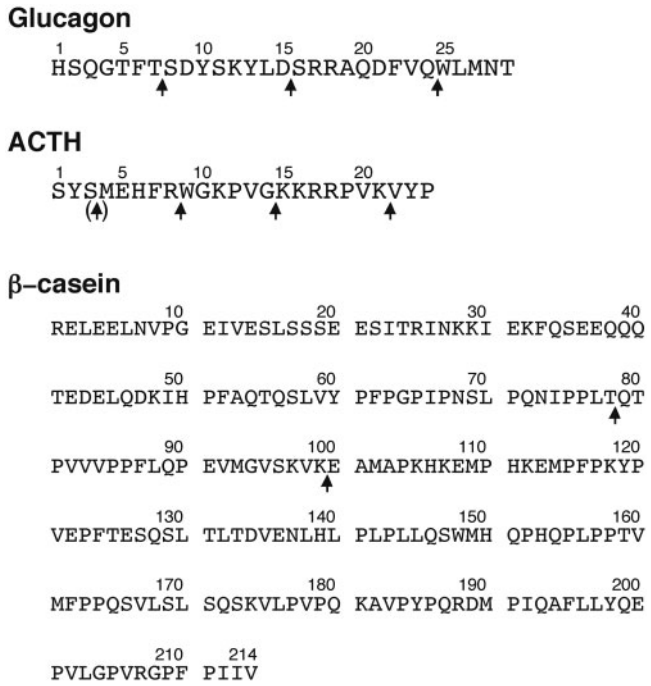

Fig. 7. **mRD21 cleavage sites located within glucagon, ACTH and β-casein.** The digest was analysed as described under MATERIALS AND METHODS section. The major cleavage sites are indicated by arrows. The arrow in parenthesis indicates a minor cleavage site.

Table 2. **Effect of various cysteine protease inhibitors on RD21 activity.**

Protease inhibitor	Concentration	Inhibition (%)	
		mRD21	iRD21
Leupeptin	1 μM	90.2	81.2
Antipain	1 μM	85.5	69.9
E-64	1 μM	85.5	70.3
CA074	10 μM	12.5	4.9
CA074	100 μM	23.6	19.3
Cystatin	2 μg/ml	96.5	94.9
Chymostatin	1 μM	46.5	41.4
TLCK	1 μM	69.1	49.9
Iodoacetamide	1 μM	5.5	18.7
PMSF	1 mM	22.1	7.3
o-phenanthroline	1 mM	26.2	5.0
EDTA	10 mM	2.6	4.0

Activity toward Z-Phe-Arg-MCA was assayed at pH 5.5 in the presence of various inhibitors.

The change in RD21 enzyme activity was analysed by DEAE-cellulose column chromatography. Three enzymes, oligopeptidase B, cathepsin B-like cysteine protease and RD21, which can hydrolyse Z-Phe-Arg-MCA, were present in the cotyledon extract. These enzymes could be separated by step-wise elution using NaCl (Fig. 8A). Three peaks with activity were eluted using 50 mM, 150 mM and 400 mM NaCl. Enzyme activities using Z-Phe-Arg-MCA and Boc-Leu-Arg-Arg-MCA as substrates were assayed to characterize these enzymes. Furthermore, the sensitivity against various inhibitors was also examined. The activity ratio (Z-Phe-Arg-MCA/Boc-Leu-Arg-Arg-MCA) of each peak differed significantly and these individual values remained unchanged for the 3, 5 and 8 day samples (peak 1: 1.4, peak 2: 0.5 and peak 3: 10). Both activities in the first peak, which were completely inhibited by leupeptin but not by E-64, eluted as a single peak at a position corresponding to a molecular mass of 80 kDa with Sephacryl S-200 chromatography, as with oligopeptidase B (*27*). These results strongly suggest that the first peak is an oligopeptidase B. In contrast, the activities of the second and third peaks were completely inhibited by E-64 or cystatin, indicating that both enzymes are papain-like cysteine proteases. As mentioned in MATERIALS AND METHODS section, elution of RD21 with DEAE-cellulose chromatography required high concentrations of NaCl (0.3–0.4 M). Furthermore, the activity ratio (Z-Phe-Arg-MCA/Boc-Leu-Arg-Arg-MCA) of purified mRD21 was almost identical to that of peak 3. Additionally, peak 3 eluted as a single peak at a position corresponding to a molecular mass of 30 kDa with Sephacryl S-100 chromatography, as was the case with purified RD21 (data not shown). Peak 2 eluted slightly slower than peak 3 with Sephacryl S-200 chromatography, suggesting that the molecular mass of the cysteine protease in peak 2 is smaller compared with that of peak 3. The sequences of the cystatin-sepharose binding proteins in peak 2 and peak 3 were determined. The N-terminal sequences of the cystatin-sepharose binding proteins of peaks 2 (28 kDa) and 3 (30 kDa) were LPKSFDA and DAIPE, respectively. The former sequence showed the highest degree of identity with cathepsin B-like cysteine protease (*Arabidopsis* CBCP: LPKAFDA, DDBJ accession number AF370193), while the latter sequence perfectly matched the N-terminal sequence of purified RD21. Thus, the enzymatic properties and sequence data indicate that the third peak is RD21 and the second peak is a cathepsin B-like cysteine protease. As shown in Fig. 8B, the enzyme activity of RD21 (peak 3) increased markedly (5.7-fold) between 3 days and 5 days, although mRNA expression levels were not significantly changed. The enzyme activity of RD21 decreased slightly at 8 days, as did RD21 mRNA levels. A comparison of the changes in expression of enzyme activity and RD21 mRNA suggests that the marked elevation of RD21 enzyme activity between 3 days and 5 days is caused post-translationally. It is highly likely that RD21 enzyme activity is regulated by autocatalytic activation in the early stage of germination, although RD21 mRNA expression was initiated by imbibition.

DISCUSSION

Recent studies have shown the involvement of plant cysteine proteases in various physiological processes such as programmed cell death (*28–30*) and disease resistance (*14*) in addition to the processing and degradation of storage proteins (*1–4*). However, the enzymatic properties of these enzymes have been poorly understood given the difficulties associated with the purification of these enzymes and subsequent expression of active recombinant enzymes. Information concerning cleavage specificities of these proteases is essential to understanding the

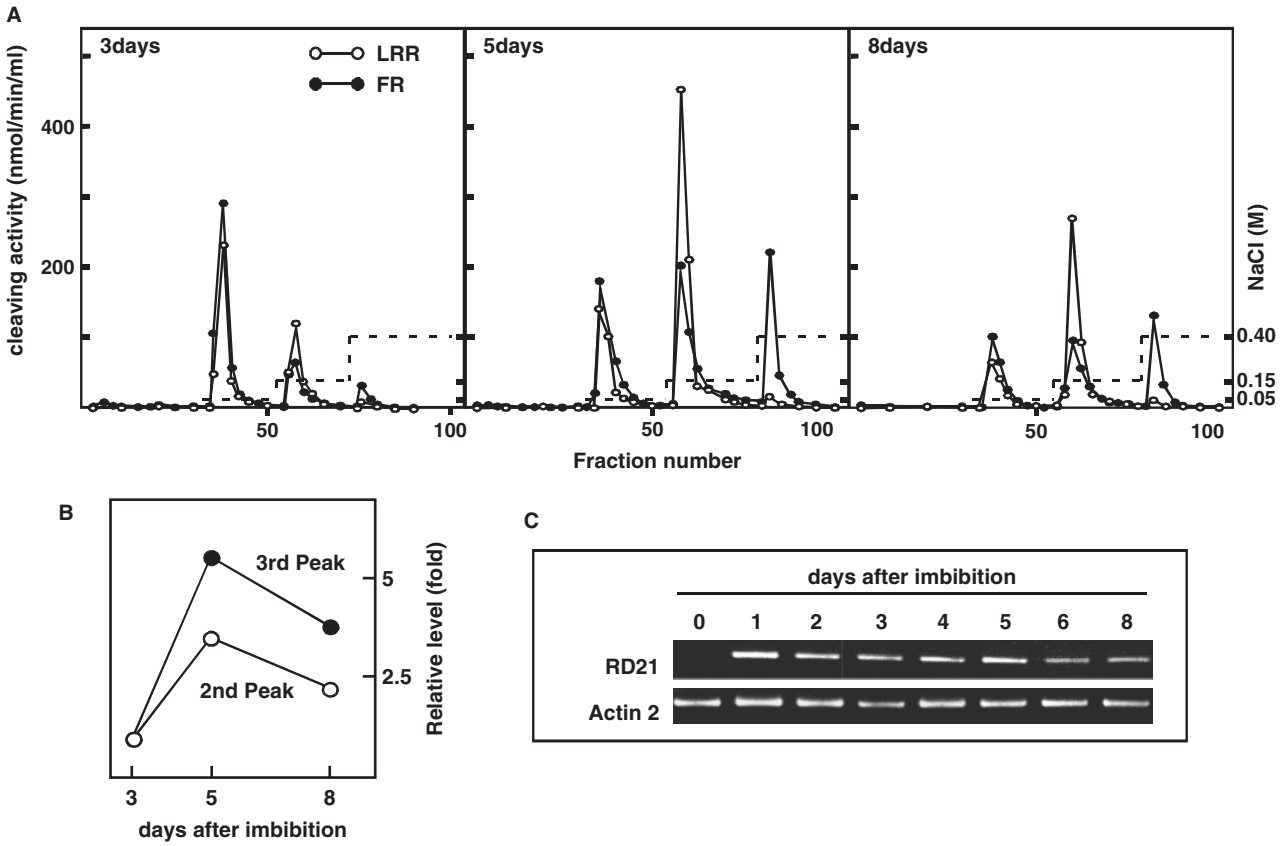

Fig. 8. **Expression analysis of daikon RD21 during germination.** (A) Homogenates of daikon radish cotyledons at 3, 5 and 8 days after imbibition were applied to a DEAE-cellulose column (2.5 × 8 cm) equilibrated with buffer A. The Z-Phe-Arg-MCA (closed circle) and Boc-Leu-Arg-Arg MCA (open circle) cleaving activities at pH 5.5 were assayed. (B) The activity towards Z-Phe-Arg-MCA in the second and third peaks in (A) are plotted against days after imbibition. (C) Total RNA was isolated from daikon radish cotyledons at 0, 1, 2, 3, 4, 5, 6 and 8 days after imbibition and analysed by RT-PCR using RD21-specific primers as described under MATERIALS AND METHODS section. Actin-2 transcript was amplified as an internal control. The amount of cDNA used as a template in the RT-PCR reactions was normalized using actin-2.

physiological role of these proteases. In this study, we initially determined the cleavage specificity of an RD21 orthologue purified from the cotyledons of daikon radish. Furthermore, we isolated iRD21 and showed that the iRD21 formed active oligomer by gel filtration and sedimentation analysis.

Although purified daikon RD21 hydrolysed synthetic substrates possessing an arginine or lysine residue at the P1 position, it had relatively strict cleavage specificity against synthetic MCA substrates. Z-Phe-Arg-MCA, Boc-Val-Leu-Lys-MCA and Z-Arg-Arg-MCA were good substrates for the enzyme, unlike the case with tri-peptide substrates such as Boc-Leu-Arg-Arg-MCA and Boc-Phe-Ser-Arg-MCA. In contrast, the enzyme exhibited broad cleavage specificity towards model peptides. Analysis of amino acid sequences around the cleavage site showed that daikon RD21 prefers aromatic and hydrophobic residues at the P2 position, while the presence of a polar amino acid such as Tyr, Thr, Asp, Gln, Lys or Arg at the P1 position enhanced the cleavage susceptibility of the peptide bond.

Previously, RD21 protein was identified as 38 kDa (iRD21) and 33 kDa (mRD21) proteins by immunoprecipitation (*20*), and as a 30 kDa protein by biotinylated E-64 labelling followed by mass spectrometry (*31*). The iRD21 accumulates in the vacuoles as an aggregate, which then slowly matures to the soluble enzyme (mRD21) following removal of the C-terminal extension sequence during leaf senescence (*20*). However, it was still unclear whether iRD21, which possesses the granulin domain, was active. In cotyledons of daikon radish, RD21 is present as iRD21 and mRD21, just as with *Arabidopsis* RD21. Gel filtration and sedimentation analyses showed that iRD21 formed aggregates which possess enzyme activity towards synthetic substrates. Major aggregate forms of iRD21 were determined to involve trimers and tetramers. The cleavage specificities of iRD21 and mRD21 towards synthetic substrates were almost identical. Both enzymes efficiently cleaved Z-Phe-Arg-MCA, Boc-Val-Leu-Lys-MCA and Z-Arg-Arg-MCA, although the K_m of these substrates for iRD21 was higher (2- to 5-fold) compared to that of mRD21. On the other hand, the cleavage specificity of the 40 kDa maize cysteine protease (CPPIC) possessing the granulin domain has been reported (*32*). Recombinant CPPIC showed strict cleavage specificity towards synthetic substrates and specific digestion of Boc-Val-Leu-Lys-MCA. Since Z-Phe-Arg-MCA and Z-Arg-Arg-MCA were not tested, the activities towards these substrates

were unclear. The aforementioned substrate specificity is very similar to that of daikon iRD21 and mRD21. Thus, taken together, the results indicate that iRD21 is active towards small synthetic substrates although its activity towards protein substrates has yet to be determined. If the active site of RD21 is masked by aggregation and iRD21 is inactive towards protein substrates, a granulin-mediated aggregation of RD21 might represent a novel regulatory mechanism of proteases as proposed by Yamada *et al*. (*20*). Further analysis of the action of iRD21 and mRD21 towards protein substrates is necessary.

Daikon RD21 mRNA was not detected in cotyledons of dormant seeds. Expression of daikon RD21 mRNA in the cotyledons was initiated by imbibition, although the expression level was almost constant during germination. In contrast, RD21 enzyme activity showed marked elevation between 3 days and 5 days after imbibition. It is highly likely that the increase in RD21 enzyme activity (5.7-fold) is regulated post-transcriptionally. Yamada *et al*. (*20*) reported that accumulation of *Arabidopsis* iRD21 was first observed 2 days after seed germination, and that iRD21 expression levels were much higher than mRD21 levels in seedlings. On the other hand, mRD21 accumulated extensively in senescence leaves. Therefore, it was suggested that RD21 plays a role in the degradation of cellular proteins during leaf senescence rather than playing a role in the degradation of seed storage proteins after germination. Similarly, daikon iRD21 expression levels were higher than mRD21 levels in cotyledons 8 days after imbibition. Our studies indicate that mRD21 possesses strong endopeptidase activity and broad cleavage specificity. The k_{cat}/K_m obtained for the hydrolysis of Z-Phe-Arg-MCA by daikon mRD21 was $1.4 \times 10^6\,M^{-1}\,s^{-1}$. This value is comparable with the k_{cat}/K_m of papain ($1.76 \times 10^6\,M^{-1}\,s^{-1}$) (*33*). Furthermore, we showed that daikon iRD21 is an active enzyme, although it is likely that the specific activity of iRD21 is lower than that of mRD21. Thus, these results suggest that RD21 plays a role in the degradation of storage proteins together with cathepsin B-like cysteine protease in seedlings after germination. Future work will focus on determining the cleavage activity of RD21 towards storage proteins and delineating the role of the granulin domain in the regulation of RD21 activity.

ACKNOWLEDGEMENTS

The authors wish to thank Ms Yuka Sasaki for determination of the amino acid sequences.

CONFLICT OF INTEREST

None declared.

REFERENCES

1. Fischer, J., Becker, C., Hillmer, S., Horstmann, C., Neubohn, B., Schlereth, A., Senyuk, V., Shutov, A., and Müntz, K. (2000) The families of papain- and legumain-like cysteine proteinases from embryonic axes and cotyledons of *Vicia* seeds: developmental patterns, intracellular localization and functions in globulin proteolysis. *Plant Mol. Biol.* **43**, 83–101
2. Gruis, D., Schulze, J., and Jung, R. (2004) Storage protein accumulation in the absence of vacuolar processing enzyme family of cysteine proteases. *Plant Cell* **16**, 270–290
3. Muramatsu, M. and Fukazawa, C. (1993) A high-order structure of plant storage proprotein allows its second conversion by an asparagine-specific cysteine protease, a novel proteolytic enzyme. *Eur. J. Biochem.* **215**, 123–132
4. Kato, H. and Minamikawa, T. (1996) Identification and characterization of a rice cysteine endopeptidase that digests glutelin. *Eur. J. Biochem.* **239**, 310–316
5. Bottari, A., Capocchi, A., Fontanini, D., and Galleschi, L. (1996) Major proteinase hydrolysing gliadin during wheat germination. *Phytochemistry* **43**, 39–44
6. Holwerda, B.C., Galvin, N.J., Baranski, T.J., and Rogers, J.C. (1990) In vitro processing of aleurain, a barley vacuolar thiol protease. *Plant Cell* **2**, 1091–1106
7. Watanabe, H., Abe, K., Emori, Y., Hosoyama, H., and Arai, S. (1991) Molecular cloning and gibberellin-induced expression of multiple cysteine proteinases of rice seeds (Oryzains). *J. Biol. Chem.* **266**, 16897–16902
8. Pechan, T., Jiang, B., Steckler, D., Ye, L., Lin, L., Luthe, D.S., and Williams, W.P. (1999) Characterization of three distinct cDNA clones encoding cysteine proteinases from maize (*Zea mays* L.) callus. *Plant Mol. Biol.* **40**, 111–119
9. Ling, J., Kojima, T., Shiraiwa, M., and Takahara, H. (2003) Cloning of two cysteine proteinase genes, *CysP1* and *CysP2*, from soybean cotyledons by cDNA representational difference analysis. *Biochim. Biophys. Acta* **1627**, 129–139
10. Yamada, K., Shimada, T., Kondo, M., Nishimura, M., and Hara-Nishimura, I. (1999) Multiple functional proteins are produced by cleaving Asn-Gln bonds of a single precursor by vacuolar processing enzyme. *J. Biol. Chem.* **274**, 2563–2570
11. Hiraiwa, N., Kondo, M., Nishimura, M., and Hara-Nishimura, I. (1997) An aspartic endopeptidase is involved in the breakdown of propeptides of storage proteins in protein-storage vacuoles of plants. *Eur. J. Biochem.* **246**, 133–141
12. Noh, Y. and Amasino, R.M. (1999) Identification of a promoter region responsible for the senescence-specific expression of *SAG12*. *Plant Mol. Biol.* **41**, 181–194
13. Chen, G., Huang, L., Yap, M., Lee, R., Huang, Y., Cheng, M., and Chen, S.G. (2002) Molecular characterization of a senescence-associated gene encoding cysteine proteinase and its gene expression during Leaf senescence in sweet potato. *Plant Cell Physiol.* **43**, 984–991
14. Krüger, J., Thomas, C.M., Golstein, C., Dixon, M.S., Smoker, M., Tang, S., Mulder, L., and Jones, J.D.G. (2002) A tomato cysteine protease required for *Cf-2*-dependent disease resistance and suppression of autonecrosis. *Science* **296**, 744–747
15. Pechan, T., Ye, L., Chang, Y., Mitra, A., Lin, L., Davis, F.M., Williams, W.P., and Luthe, D.S. (2000) A unique 33-kD cysteine proteinase accumulates in response to larval feeding in maize genotypes resistant to fall armyworm and other lepidoptera. *Plant Cell* **12**, 1031–1040
16. Konno, K., Hirayama, C., Nakamura, M., Tateishi, K., Tamura, Y., Hattori, M., and Kohno, K. (2004) Papain protects papaya trees from herbivorous insects: role of cysteine proteases in latex. *Plant J.* **37**, 370–378
17. Koizumi, M., Yamaguchi-Shinozaki, K., Tsuji, H., and Shinozaki, K. (1993) Structure and expression of two genes that encode distinct drought-inducible cysteine proteinases in *Arabidopsis Thaliana*. *Gene* **129**, 175–182
18. Yamaguchi-Shinozaki, K., Koizumi, M., Urao, S., and Shinozaki, K. (1992) Molecular cloning and characterization of 9 cDNAs for genes that are responsive to desiccation in *Arabidopsis Thaliana*: sequence analysis of one cDNA clone that encodes a putative transmembrane channel protein. *Plant Cell Physiol.* **33**, 217–224
19. Gepstein, S., Sabehi, G., Carp, M., Hajouj, T., Nesher, M.F.O., Yariv, I., Dor, C., and Bassani, M. (2003)

Large-scale identification of leaf senescence-associated genes. *Plant J.* **36**, 629–642
20. Yamada, K., Matsushima, R., Nishimura, M., and Hara-Nishimura, I. (2001) A slow maturation of a cysteine protease with a granulin domain in the vacuoles of senescing Arabidopsis leaves. *Plant Physiol.* **127**, 1626–1634
21. Hayashi, Y., Yamada, K., Shimada, T., Matsushima, R., Nishizawa, N.K., Nishimura, M., and Hara-Nishimura, I. (2001) A proteinase-storing body that prepares for cell death or stresses in the epidermal cells of Arabidopsis. *Plant Cell Physiol.* **42**, 894–899
22. Anastasi, A., Brown, M.A., Kembhavi, A.A., Nicklin, M.J.H., Sayers, C.A., Sunter, D.C., and Barrett, A.J. (1983) Cystatin, a protein inhibitor of cysteine proteinases. Improved purification from egg white, characterization, and detection in chicken serum. *Biochem. J.* **211**, 129–138
23. Tombaccini, D., Mocali, A., Weber, E., and Paoletti, F. (2001) A cystatin-based affinity procedure for the isolation and analysis of papain-like cysteine proteinases from tissue extracts. *Anal. Biochem.* **289**, 231–238
24. Tsuji, A. and Kurachi, K. (1989) Isolation and characterization of a novel large protease accumulated in mammalian cells in the presence of inhibitors. *J. Biol. Chem.* **264**, 16093–16099
25. Bradford, M.M. (1976) A rapid and sensitive method for the quantitation of microgram quantities of protein utilizing the principle of protein-dye binding. *Anal. Biochem.* **72**, 248–254
26. Laemmli, U.K. (1970) Cleavage of structural proteins during the assembly of the head of bacteriophage T4. *Nature* **227**, 680–685
27. Tsuji, A., Yuasa, K., and Matsuda, Y. (2004) Identification of oligopeptidase B in higher plants. Purification and characterization of oligopeptidase B from quiescent wheat embryo, *Triticum aestivum*. *J. Biochem.* **136**, 673–681
28. Solomon, M., Belenghi, B., Delledonne, M., Menachem, E., and Levine, A. (1999) The involvement of cysteine proteases and protease inhibitor genes in the regulation of programmed cell death in plants. *Plant Cell* **11**, 431–443
29. Beers, E.P., Woffenden, B.J., and Zhao, C. (2000) Plant proteolytic enzymes: possible roles during programmed cell death. *Plant Mol. Biol.* **44**, 399–415
30. Funk, V., Kositsup, B., Zhao, C., and Beers, E.P. (2002) The Arabidopsis xylem peptidase XCP1 is a tracheary element vacuolar protein that may be a papain ortholog. *Plant Physiol.* **128**, 84–94
31. Van der Hoorn, R.A.L., Leeuwenburgh, M.A., Bogyo, M., Joosten, M.H.A.J., and Peck, S.C. (2004) Activity profiling of papain-like cysteine proteases in plants. *Plant Physiol.* **135**, 1170–1178
32. Yamada, T., Ohta, H., Shinohara, A., Iwamatsu, A., Shimada, H., Tsuchiya, T., Masuda, T., and Takamiya, K. (2000) A cysteine protease from maize isolated in a complex with cystatin. *Plant Cell Physiol.* **41**, 185–191
33. Meara, J.P. and Rich, D.H. (1995) Measurement of individual rate constants of irreversible inhibition of a cysteine proteinase by an epoxysuccinyl inhibitor. *Bioorg. Med. Chem. Lett.* **5**, 2277–2282